VOLUME 25 NUMBER 2

ACCOUNTS OF CHEMICAL RESEARCH®

FEBRUARY 1992

Surface-Bound Metal Hydrocarbyls. Organometallic Connections between Heterogeneous and Homogeneous Catalysis

TOBIN J. MARKS

Department of Chemistry, Northwestern University, Evanston, Illinois 60208-3113

Received August 5, 1991 (Revised Manuscript Received November 25, 1991)

Many key transformations in heterogeneous catalysis involve the creation or modification of surface metal–hydrocarbyl (alkyl, aryl, etc.) functionalities. One attractive approach to characterizing such highly reactive species is to create them by adsorption of well-defined molecular precursors onto carefully prepared inorganic surfaces.[1,2] For several classes of early transition metal hydrocarbyls, it has been known since the 1960s that adsorption on high surface area metal oxides is accompanied by dramatic enhancements in activity for olefin transformations such as polymerization and metathesis.[1,3,4] The study of such materials is of both fundamental scientific significance (What unique surface coordination environments give rise to such enhancements in chemical reactivity?) and technological interest (What clues are offered regarding the nature of highly efficient third-generation Ziegler–Natta olefin polymerization catalysts? Is it possible to "tailor" catalysts for improved chemo-, regio-, and stereoselectivity?). Despite these motivations and much empirical data, it is fair to say that our understanding of the overall surface coordination chemistry as well as the precise nature of the catalytically active sites has been at a very primitive level.

The purpose of this Account is to review recent supported metal hydrocarbyl research carried out at Northwestern University. The goal has been to build bridges between the unusual surface organometallic chemical/heterogeneous catalytic properties of adsorbed, well-defined metal hydrocarbyls and the phenomenology of contemporary molecular organometallic chemistry. Initial subjects were organoactinide molecules, since the chemistry, spectroscopy, and thermochemistry of such species are reaching an instructive level of sophistication.[5] Moreover, isostructural adsorbed Th(IV) ($5f^0$) and U(IV) ($5f^2$) species offer an informative comparison. While 4+ is virtually the only known oxidation state in Th organometallic chemistry (oxidation is impossible; reduction is exceedingly dif-

Tobin J. Marks received his B.S. degree from the University of Maryland in 1966 and his Ph.D. from MIT in 1970 under F. A. Cotton. He has been at Northwestern University since 1970 and is currently Charles E. and Emma H. Morrison Professor of Chemistry as well as Professor of Materials Science and Engineering. His research interests include synthetic and mechanistic f- and d-element organometallic chemistry, catalysis, nonlinear optical materials, new types of superconductors, synthetic metals, and metal complexes with carcinostatic properties.

(1) For leading review references in this area, see: (a) Iwasawa, Y.; Gates, B. C. *CHEMTECH* **1989**, 173–181 and references therein. (b) Basset, J. M., et al., Eds. *Surface Organometallic Chemistry: Molecular Approaches to Surface Catalysis*; Kluwer: Dordrecht, 1988. (c) Hartley, F. R. In *The Chemistry of the Metal-Carbon Bond*; Hartley, F. R., Ed.; Wiley: New York, 1987; Vol. 4, pp 1164–1225. (d) Yermakov, Y. I.; Kuznetsov, B. N.; Zakharov, V. A. *Catalysis by Supported Complexes*; Elsevier: Amsterdam, 1981.

(2) (a) Lee, F. R.; Whitesides, G. M. *J. Am. Chem. Soc.* **1991**, *113*, 2576–2585 and references therein. (b) Schwartz, J. *Acc. Chem. Res.* **1985**, *18*, 302–308.

(3) (a) Quirk, R. P., Ed. *Transition Metal Catalyzed Polymerizations*; Cambridge University Press: Cambridge, 1988. (b) Kaminsky, W., Sinn, H., Eds. *Transition Metals and Organometallics as Catalysts for Olefin Polymerization*; Springer: New York, 1988. (c) Keii, T., Soga, K. Eds. *Catalytic Polymerization of Olefins*; Elsevier: Amsterdam, 1986. (d) McDaniel, M. P. *Adv. Catal.* **1985**, *33*, 47–98.

(4) (a) Tullock, C. W.; Tebbe, F. N.; Mulhaupt, R.; Ovenall, D. W.; Setterquist, R. A.; Ittel, S. D. *J. Polym. Sci., Part A: Polym. Chem.* **1989**, *27*, 3063–3081. (b) Xiaoding, X.; Boelhouwer, C.; Vonk, D.; Benecke, J. I.; Mol, J. C. *J. Mol. Catal.* **1986**, *36*, 47–66 and references therein. (c) Karol, F. J. *Catal. Rev.—Sci. Eng.* **1984**, *26*, 557–595. (d) Firment, L. E. *J. Catal.* **1983**, *82*, 196–212 and references therein.

(5) (a) Marks, T. J.; Streitwieser, A., Jr. In *The Chemistry of the Actinide Elements*, 2nd Ed.; Katz, J. J., Seaborg, G. T., Morss, L. R., Eds.; Chapman and Hall: London, 1986; Chapter 22. (b) Marks, T. J. *Ibid.*; Chapter 23.

0001-4842/92/0125-0057$03.00/0

ficult[6]), a multiplicity of states is available for U.[5] Hence, the facility of oxidative addition/reductive elimination sequences, key transformations in transition-metal organometallic chemistry, should be greatly different for catalytic centers derived from Th and U precursors. Furthermore, the unpaired 5f electrons of U(IV) provide a useful NMR spectroscopic probe.

We begin with a discussion of inorganic supports as ligands, followed by a summary of organoactinide surface chemical and heterogeneous catalytic observations. While these results are informative in regard to the adsorption process and establishing high catalytic activity, they also illustrate the elusive character of surface adsorbate structural information in situations not readily addressed by contemporary surface photon/particle absorption or scattering techniques. We then show how high-resolution solid-state NMR spectroscopy provides a definitive picture of adsorbate structure and reactivity as well as clues to developing functional homogeneous model chemistry. Finally, we generalize these results to group 4 surface and solution chemistry.

Inorganic Surfaces as Ligands

The surface chemistry of γ-alumina typifies that of many metal oxides in that heating eliminates water at the expense of surface OH functionalities (schematized in eq 1).[7] In the case of PDA (partially dehydroxylated

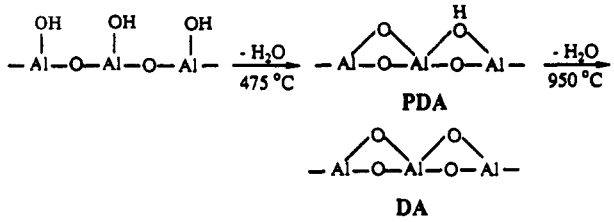

(1)

alumina), ~4 Brønsted acidic OH groups, ~5.5 Lewis acidic Al^{3+} centers, and ~5.5 Lewis basic oxide groups remain per square nanometer of surface area. For DA, the corresponding populations are ~0.12, ~5.5, and ~5.5, respectively. Both PDA and DA have surface areas of ~160 m^2/g. From the standpoint of coordination chemistry, the availability of *both basic and acidic ligation sites* provides a unique complexation environment. Silica differs from alumina in that the surface OH groups are somewhat more acidic, no Lewis acid sites are present, and the -Si-O- bonds are probably weaker.[7] $MgCl_2$ is a common support for third-generation Ziegler–Natta catalysts, has a CdI_2 crystal structure, and has a surface offering both Lewis acidic (Mg^{2+}) and basic (Cl^-) functionalities.[8] Typical surface areas are ~250 m^2/g.

(6) (a) Kot, W. K.; Shalimoff, G. V.; Edelstein, N. M.; Edelman, M. A.; Lappert, M. F. *J. Am. Chem. Soc.* **1988**, *110*, 986–987 and references therein. (b) Bruno, J. W.; Kalina, D. G.; Mintz, E. A.; Marks, T. J. *J. Am. Chem. Soc.* **1982**, *104*, 1860–1869. (c) Vallat, A.; Laviron, E.; Dormond, A. *J. Chem. Soc., Dalton Trans.* **1990**, 921–924.

(7) (a) Kijenski, J.; Baiker, A. *Catal. Today* **1989**, *5*(1), 1–120. (b) Beránek, L.; Kraus, M. In *Comprehensive Chemical Kinetics*; Bamford, C. H., Tipper, C. F. H., Eds.; Elsevier: Amsterdam, 1978; Vol. 20, pp 263–398. (c) Benesi, H. A.; Winquist, B. H. C. *Adv. Catal.* **1978**, *27*, 97–182. (d) Knözinger, H.; Ratnasamy, P. *Catal. Rev.—Sci. Eng.* **1978**, *17*, 31–70.

(8) (a) Wells, A. F *Structural Inorganic Chemistry*, 5th ed.; Oxford, University Press: New York, 1984; p 350. (b) Marigo, A.; Martorana, A.; Zannetti, R. *Makromol. Chem., Rapid Commun.* **1987**, *8*, 65–68. (c) Bassi, I. W.; Polato, F.; Calcaterra, M.; Bart, J. C. J. *Z. Kristallogr.* **1982**, *159*, 297–302 and references therein.

Organoactinide Surface Chemistry and Heterogeneous Catalysis

Studies of organoactinide surface chemistry and catalysis have been carried out under rigorously anhydrous/anaerobic conditions at coverages of ~0.25–0.50 molecules/nm^2.[9] As indicated by product yields, isotopic labeling, and surface reactivity, the irreversible γ-alumina adsorption chemistry of $Cp'_2An(CH_3)_2$ complexes ($Cp' = \eta^5$-$(CH_3)_5C_5$; An = Th, U) is describable by three methane-evolving pathways (eqs 2–4). Path-

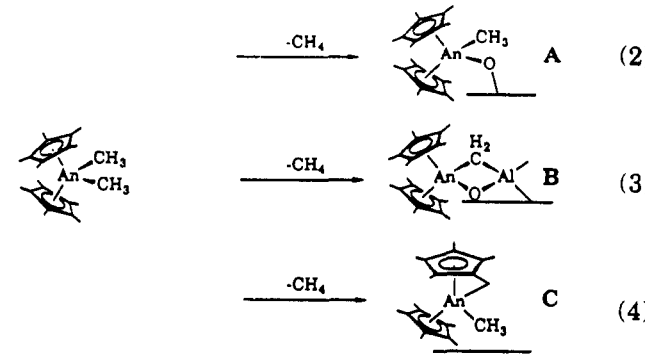

way 2 dominates adsorption on PDA. On DA, however, pathways 2–4 account for ≲16% of all available An–CH_3 groups (B can also be assayed via methylene transfer reactivity[9]). That is, the majority of methyl groups remain bound to the surface in some way not revealed by these chemical experiments. Chemical probes such as H_2 (or D_2) reveal that an additional ~10–20% of the methyl groups can be liberated by hydrogenolysis (eq 5). The virtually indistinguishable

$$AnCH_3 + H_2(D_2) \rightarrow AnH(D) + CH_4(CH_3D) \quad (5)$$

behavior of $Cp'_2Th(CH_3)_2$ and $Cp'_2U(CH_3)_2$ in these experiments argues that change in metal oxidation state is not an important part of the adsorption chemistry. There is no evidence for significant Cp'H liberation.

Although complexes such as $Cp'_2Th(CH_3)_2$ are marginally active for olefin hydrogenation and ethylene polymerization in homogeneous solution,[10] adsorption upon DA results in a dramatic enhancement in catalytic activity. With propylene hydrogenation as a probe reaction, kinetic experiments reveal catalytic activities comparable to those of heterogeneous platinum metal catalysts.[9a,11] A common characteristic of heterogeneous catalysts is that only a fraction of the surface sites are catalytically significant. For the $Cp'_2An(CH_3)_2$/DA, quantitative poisoning studies using either CO, H_2O, or CH_3Cl as probes, reveal that stoichiometrically small amounts of these poisons (corresponding to ~4% of available actinide sites) completely suppress catalytic activity. That is, only ~4% of the $Cp'_2Th(CH_3)_2$/DA sites sustain the bulk of the hydrogenation activity. *These remarkable sites then have turnover frequencies for propylene hydrogenation greater than the active*

(9) (a) He, M.-Y.; Xiong, G.; Toscano, P. J.; Burwell, R. L., Jr.; Marks, T. J. *J. Am. Chem. Soc.* **1985**, *107*, 641–652. (b) He, M.-Y.; Burwell, R. L., Jr.; Marks, T. J. *Organometallics* **1983**, *2*, 566–569.

(10) (a) Fendrick, C. M.; Schertz, L. D.; Day, V. W.; Marks, T. J. *Organometallics* **1988**, *7*, 1828–1838. (b) Fagan, P. J.; Manriquez, J. M.; Maatta, E. A.; Seyam, A. M.; Marks, T. J. *J. Am. Chem. Soc.* **1981**, *103*, 6650–6667.

(11) (a) Gillespie, R. D.; Burwell, R. L., Jr.; Marks, T. J. *Langmuir* **1990**, *6*, 1465–1477. (b) Burwell, R. L., Jr.; Marks, T. J. In *Catalysis of Organic Reactions*; Augustine, R. L., Ed.; Marcel Dekker, Inc.: New York, 1985; pp 207–224.

sites of Pt/SiO_2[12] *under the same conditions* ($N_t \approx 2$ s^{-1} vs 0.05 s^{-1} at −63 °C). Kinetic/mechanistic studies of $Cp'_2Th(CH_3)_2$/DA-catalyzed propylene hydrogenation are in accord with the sequence in eqs 6 and 7, where the rate law is zero-order in olefin, hydrogen delivery to propylene is regiospecifically 1,2, E_a = 3.6(2) kcal/mol, and $N_t(H_2)/N_t(D_2)$ = 1.5(1). Regarding eq

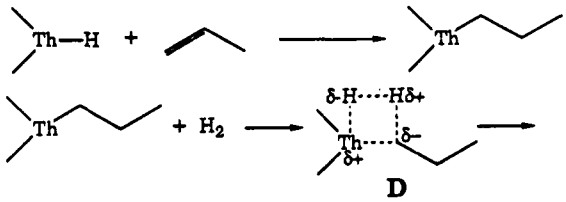

D

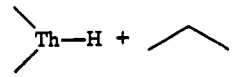

7, there is ample precedent for facile cleavage of metal–alkyl bonds via "heterolytic" four-center transition states (D)[10b,13] not involving oxidative addition/reduction elimination sequences. It is noteworthy that many aspects of this surface chemistry and catalysis are analogous to homogeneous catalysis by coordinatively unsaturated organolanthanide complexes (E)[14] as well as stoichiometric solution olefin addition[15a] and hydrocarbyl hydrogenolysis chemistry.[15b] Nevertheless, chemical and catalytic data reveal little concerning the actual structures of the surface active sites.

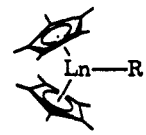

E

As a function of support, the activities of adsorbed $Cp'_2Th(CH_3)_2$ heterogeneous propylene hydrogenation catalysts roughly follow the ordering of support Lewis acidity:[7,11a]

$$DA > SiO_2\text{–}Al_2O_3 > MgCl_2 \gg PDA, MgO, SiO_2$$

In contrast to the $Cp'_2Th(CH_3)_2$/DA results, poisoning experiments reveal that 40 ± 10% of $Cp'_2Th(CH_3)_2$/$MgCl_2$ sites are catalytically significant. The inactivity of $Cp'_2Th(CH_3)_2$/PDA is consistent with the low electrophilicity (due to heteroatom lone pair donation, F) and sluggish olefin insertion/hydrogenolysis of alkoxyalkyls such as A.[15] How $Cp'_2Th(CH_3)_2$ adsorbs on

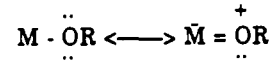

F

rigorously dehydroxylated SiO_2 to yield a catalytically inert adsorbate is not obvious from these data. As a function of precursor, propylene hydrogenation activities on DA approximately parallel the coordinative unsaturation of the precatalyst (R = alkyl and/or hydride; Cp = η^5-C_5H_5):[11a,16]

$$Th(\eta^3\text{-allyl})_4 > Cp'ThR_3 > Cp'_2ThR_2 > Cp_3ThR$$

$Th(\eta^3$-allyl$)_4$/DA is an active arene hydrogenation catalyst (rivaling platinum metal catalysts in activity),[16] while N_t for $Cp'Th(benzyl)_3$/DA-catalyzed propylene hydrogenation (~20 s^{-1} at −63 °C) is comparable to that of Rh/SiO_2 active sites under the same experimental conditions. Rh/SiO_2 is the most active heterogeneous olefin hydrogenation catalyst known. Where investigated, activities for analogous Th- and U-based catalysts, and for alkyl- and hydride-based catalysts, are indistinguishable. This argues that metal oxidation state shuttling is not catalytically significant and that alkyls and hydrides form identical active sites. For all $Cp'_2An(CH_3)_2$/DA and $Cp'AnR_3$/DA catalysts examined, the percentages of catalytically important sites is invariably small (~5%). For the adsorbed $Cp'ThR_3$ and Cp'_2ThR_2 series, ethylene polymerization activities parallel propylene hydrogenation activities, and percentages of active sites are comparable. As a function of olefin, relative $Cp'_2Th(CH_3)_2$/DA catalytic hydrogenation activities are[11a]

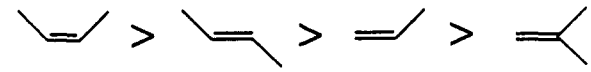

While the above results provide informative catalytic phenomenology and restrict possible mechanistic scenarios for catalytic cycles, they leave unanswered atomic-level questions about the exact nature of the molecule–surface interaction.

High-Resolution Solid-State NMR Spectroscopy of Adsorbed Metal Hydrocarbyls

The precise structural characterization of hydrocarbyls adsorbed on irregular metal oxide and halide surfaces at less than monolayer coverage presents a challenge for most physical characterization methods. While NMR spectroscopy of adsorbed systems has traditionally been frustrated by internuclear dipolar coupling, unfavorable spin–lattice relaxation times, and (for many nuclei) large chemical shift anisotropies, high-resolution CPMAS (cross polarization with magic angle spinning) techniques have dramatically altered this picture. In the present case, the high surface areas of the supports enhance achievable adsorbate concentrations. In addition, assignment aids such as isotopic labeling, model compounds, interrupted decoupling, variable magnetic fields, supports having quadrupolar nuclei, paramagnetic probes, and techniques to probe adsorbate mobility have proven invaluable. Of course, rigorously anhydrous and anaerobic sample handling techniques must be developed.

The ^{13}C CPMAS NMR spectra of $Cp'_2Th(^{13}CH_3)_2$/DA and $Cp'_2Th(^{13}CH_3)_2/MgCl_2$ can be completely assigned using the aforementioned methodology and lead to a remarkable conclusion: *a methide anion has been transferred from the actinide center to a Lewis acid site on the surface* (e.g., eq 8).[17] Thus, Al–CH_3 and Mg–CH_3 resonances appear at characteristic field positions, and the Th–$^{13}CH_3$ signal is shifted slightly

(12) Otero-Schipper, P. H.; Wachter, W. A.; Butt, J. B.; Burwell, R. L., Jr.; Cohen, J. B. *J. Catal.* **1977**, *50*, 494–507.
(13) (a) Gillespie, R. D.; Burwell, R. L., Jr.; Marks, T. J. *Catal. Lett.* **1991**, *9*, 363–368. (b) Collman, J. P.; Hegedus, L. S.; Norton, J. R.; Finke, R. G. *Principles and Applications of Organotransition Metal Chemistry*; University Science: Mill Valley, CA, 1987; Chapter 5.3. (c) Rabaâ, H.; Saillard, J. Y.; Hoffmann, R. *J. Am. Chem. Soc.* **1986**, *108*, 4327–4336.
(14) (a) Mauermann, H.; Swepston, P. N.; Marks, T. J. *Organometallics* **1985**, *4*, 200–202. (b) Jeske, G.; Lauke, H.; Mauermann, H.; Schumann, H.; Marks, T. J. *J. Am. Chem. Soc.* **1985**, *107*, 8111–8118.
(15) (a) Lin, Z.; Marks, T. J. *J. Am. Chem. Soc.* **1990**, *112*, 5515–5525. (b) Lin, Z.; Marks, T. J. *J. Am. Chem. Soc.* **1987**, *109*, 7979–7985.
(16) Eisen, M. S.; Marks, T. J. Submitted for publication.

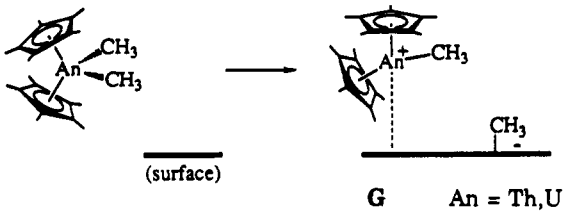

(8)

G An = Th,U

downfield as might be expected for a formally "cation-like" complex (Figure 1; G). In contrast, $Cp'_2Th(^{13}CH_3)_2$/PDA and $Cp'_2Th(^{13}CH_3)_2$/dehydroxylated silica exhibit quite different CPMAS spectra, assignable to structures H and I,[17a,18] respectively. These con-

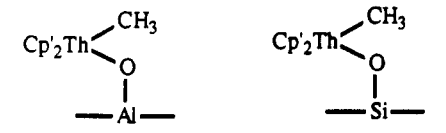

H I

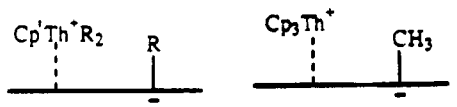

J K

clusions are supported by data for model compounds and are consistent with the aforementioned surface chemical/catalytic observations. The spectra of $Cp'Th(^{13}CH_2C_6H_5)_3$/DA and $Cp_3Th(^{13}CH_3)$/DA can likewise be assigned "cation-like" structures J and K,[17a] respectively. Several experiments indicate that adsorbate motion is not sufficiently rapid and isotropic to significantly average C–H dipolar interactions for any of the adsorbate species.

Returning to G, an obvious structural analogy to the highly active lanthanide Cp'_2MR catalysts E is evident. Moreover, the high electrophilicity attending cationic character would be expected to facilitate olefin insertion and alkyl hydrogenolysis (eqs 6 and 7).[15] Questions remain regarding residual interactions between the actinide center and the transferred methyl group (is it a μ-CH_3 complex such as L?) as well as the surface.

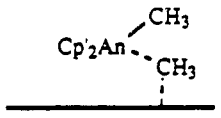

L

Since bridging alkyl groups are sometimes associated with special reactivity properties in mechanistic discussions of Ziegler–Natta catalysis,[1,3] the former question takes on particular significance. It is possible to probe the actinide···CH_3(surface) distances by making use of the large magnetic anisotropy based and unpaired spin density delocalization based chemical shift displacements that nuclei bound to paramagnetic f ions can undergo. For $Cp'_2U(^{13}CH_3)_2$, the U–$^{13}CH_3$ signals are shifted ~1410 ppm downfield vs the Th–$^{13}CH_3$ resonances of $Cp'_2Th(^{13}CH_3)_2$! CPMAS spectra of $Cp'_2U(^{13}CH_3)_2$/DA reveal that the great majority (≳90%) of the surface Al–$^{13}CH_3$ nuclei do not "feel" the

(17) (a) Finch, W. C.; Gillespie, R. D.; Hedden, D.; Marks, T. J. *J. Am. Chem. Soc.* **1990**, *112*, 6221–6232. (b) Hedden, D.; Marks, T. J. *J. Am. Chem. Soc.* **1988**, *110*, 1647–1649. (c) Toscano, P. J.; Marks, T. J. *J. Am. Chem. Soc.* **1985**, *107*, 653–659.

(18) Toscano, P. J.; Marks, T. J. *Langmuir* **1986**, *2*, 820–823.

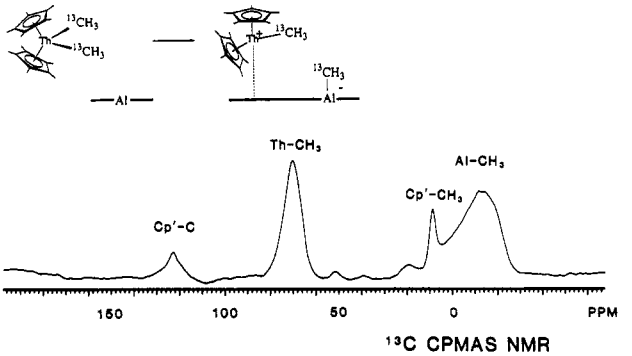

Figure 1. ^{13}C CPMAS NMR spectrum (74.5 MHz) of $Cp'_2Th(^{13}CH_3)_2$ (99% ^{13}C enrichment of methyl groups) adsorbed on dehydroxylated alumina (DA).

Scheme I
Tracing the Pathway(s) for Surface Ethylene Polymerization

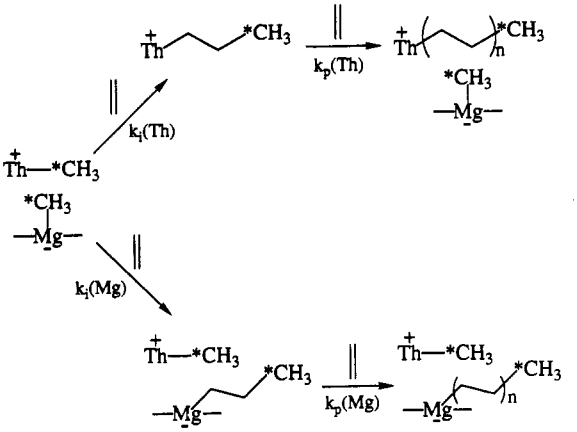

presence of the U(IV) unpaired in 5f electrons. Similar conclusions can be drawn for $Cp'_2U(^{13}CH_3)_2/MgCl_2$ and $Cp'_2U(^{13}CH_3)_2$/dihydroxylated silica, and minimum U···CH_3(surface) distances on the order of ≳5 Å are estimated.[17a] Clearly μ-CH_3 species are not a major part of this surface chemistry. The nature of the residual organoactinide–surface interaction in G (the surface is in actuality the charge-compensating counterion) is more problematic. It is likely that the irregular character of the surface topology gives rise to a variety of sterically and electronically differing surface adsorption sites.[7] This explains broad adsorbate line shapes in the NMR spectrum, as well as support-dependent differences in reactivity and percentage active sites. Models for these counterion effects will be taken up in the discussion of homogeneous models (vide infra).

What does the surface spectroscopy teach us about adsorbate reactivity? Unfortunately, the catalytic poisoning derived percentage of $Cp'_2Th(^{13}CH_3)_2$/DA active sites is to small to directly observe transformations at the adsorbate centers by NMR. For example, ethylene dosing of $Cp'_2Th(^{13}CH_3)_2$/DA produces large oligo/polyethylene signals but undetectable alterations in the oragnometallic adsorbate features. In agreement with the catalytic poisoning experiments, the percentage of sites reacting with olefin is below the NMR detection limits. However, $Cp'_2Th(^{13}CH_3)_2/MgCl_2$, in which 40 ± 10% of the sites are active for propylene hydrogenation, offers better prospects. Thus, the question of whether the site of ethylene insertion is at surface Th–$^{13}CH_3$ or Mg–$^{13}CH_3$ functionalities or at both can be

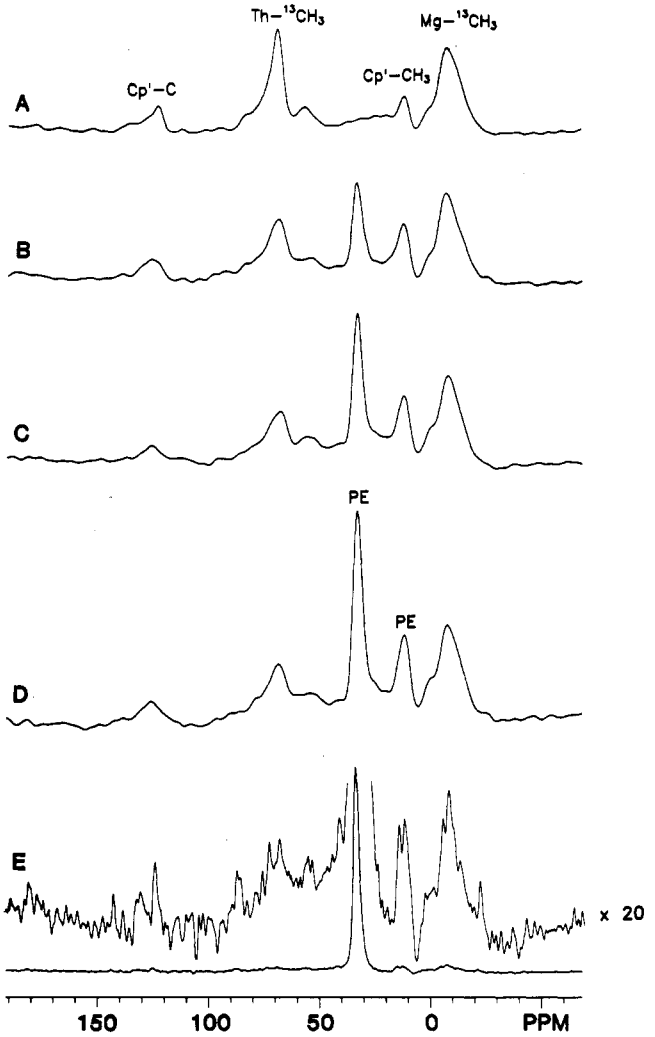

Figure 2. ^{13}C CPMAS NMR spectra (75.4 MHz) of (A) $Cp'_2Th(^{13}CH_3)_2/MgCl_2$, (B) $Cp'_2Th(^{13}CH_3)_2/MgCl_2$ exposed to 5.0 equiv of ethylene, (C) $Cp'_2Th(^{13}CH_3)_2/MgCl_2$ exposed to 10.0 equiv of ethylene, (D) $Cp'_2Th(^{13}CH_3)_2/MgCl_2$ exposed to 16.0 equiv of ethylene, and (E) $Cp'_2Th(^{13}CH_3)_2/MgCl_2$ exposed to 350 equiv of ethylene. PE denotes the location of polyethylene signals (from ref 17a).

addressed in competition studies. As illustrated in Scheme I, ethylene insertion converts the amplified (99% ^{13}C) metal–CH_3 magnetization into that of an environment characteristic of an oligoethylene end-group. Hence, spectroscopic signatures of reactive moieties should be greatly attenuated, while those of "spectator" groups remain unchanged. The actual experiment is shown in Figure 2, where $Cp'_2Th(^{13}CH_3)_2/MgCl_2$ samples are dosed with ethylene at 77 K (to allow ethylene diffusion into the catalyst pore structure prior to reaction) and then allowed to warm to room temperature. Only the Th–$^{13}CH_3$ resonance is diminished by ethylene addition. Quantitative analysis of the NMR data as a function of ethylene dosage indicates that >90 ± 10% of the ethylene insertions occur at the Th–$^{13}CH_3$ centers and that 50 ± 10% of the Th sites are reactive under the experimental conditions. The latter figure is in excellent agreement with the active-site percentage determined by catalytic poisoning (40 ± 10%). Moreover, the Th–$^{13}CH_3$ region of Figure 2 reveals an upfield shoulder ($\delta \sim 60$) that can be assignable to a μ-oxo species (e.g., A, arising from traces of surface hydroxyl groups). In competition with the

Scheme II
Catalytic Olefin Hydrogenation by Supported Organoactinide Complexes

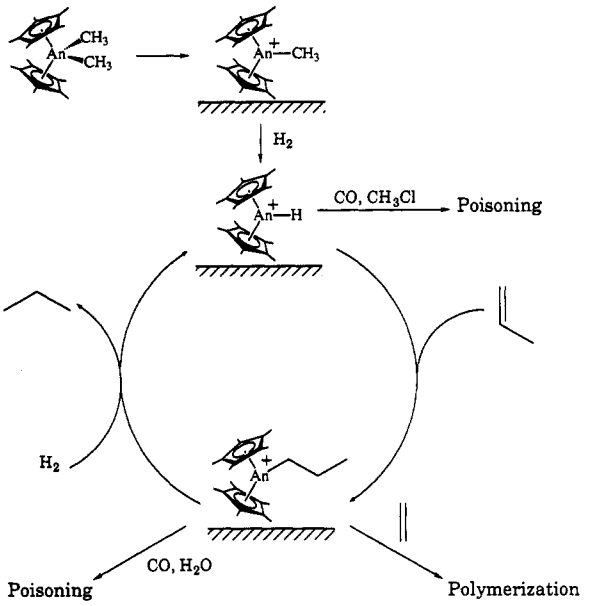

surface cation G, it can be seen that this species is unreactive, in agreement with previously discussed solution chemistry. Assuming surface ethylene oligomerization/polymerization to be a terminationless, transferless "living" sequential insertion process[19] described by single initiation and single propagation rate constants (k_i and k_p), k_p/k_i can be estimated from the spectroscopic data and the quantities of ethylene introduced. We estimate that $k_p/k_i \approx 12$, similar to $k_p/k_i \approx 7.5$ for Cp'_2ScR ethylene insertion in solution at −80 °C.[20]

NMR probing of adsorbate reactivity is not restricted to ethylene insertion. Thus, other reagents (e.g., H_2, CO, propylene) and spectroscopies (e.g., ^1H MAS) reveal a rich and intricate surface chemistry.[17] For example, $Cp'_2Th(^{13}CH_3)_2/MgCl_2$ chemistry with propylene appears to involve allylic C–H activation (eq 9), while the surface Mg–CH_3 groups undergo facile hydrogenolysis (eq 10).

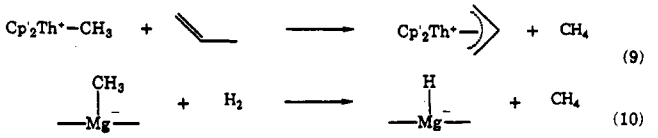

On the basis of the above catalytic and spectroscopic experiments, it is possible to propose a mechanism for the hydrogenation of simple olefins by adsorbed $Cp'_2Th(CH_3)_2$ complexes (Scheme II). In the absence of H_2, ethylene polymerization is observed, while poisoning occurs via amply precedented migratory CO insertion,[21] halocarbon/hydride metathesis,[10] or alkyl protonolysis.[10,22] The next question is to what degree

(19) (a) Watson, P. J.; Parshall, G. W. *Acc. Chem. Res.* **1985**, *18*, 51–56. (b) Jeske, G.; Lauke, H.; Mauermann, H.; Swepston, P. N.; Schumann, H.; Marks, T. J. *J. Am. Chem. Soc.* **1985**, *107*, 8091–8103. (c) Jeske, G.; Schock, L. E.; Swepston, P. N.; Schumann, H.; Marks, T. J. *J. Am. Chem. Soc.* **1985**, *107*, 8103–8110.

(20) Burger, B. J.; Thompson, M. E.; Cotter, W. D.; Bercaw, J. E. *J. Am. Chem. Soc.* **1990**, *112*, 1566–1577.

(21) (a) Tatsumi, K.; Nakamura, A.; Hofmann, P.; Hoffmann, R.; Moloy, K. G.; Marks, T. J. *J. Am. Chem. Soc.* **1986**, *108*, 4467–4476 and references therein. (b) Moloy, K. G.; Fagan, P. J.; Manriquez, J. M.; Marks, T. J. *J. Am. Chem. Soc.* **1986**, *108*, 56–67 and references therein.

Table I
^{13}C NMR Data for Surface and Model Organothorium Complexes

complex	δ Th–$^{13}CH_3$ (ppm)
$Cp'_2ThCH_3^+B(C_6F_5)_4^-$ [a]	78.1
$Cp'_2ThCH_3^+B(C_6H_5)_4^-$ [a]	71.8
$Cp'_2Th(CH_3)_2$/DA [b]	**71.0**
$Cp'_2Th(THF)_2CH_3^+B(C_6H_5)_4^-$ [a]	68.8
$Cp'_2Th(CH_3)_2$ [a,b]	68.4
$Cp'_2Th(CH_3)^+[Co(C_2B_9H_{11})_2^-]$ [a]	61.6
$Cp'_2Th(CH_3)_2$/DS [b,c]	**59.0**
$Cp'_2Th(CH_3)[OSiMe_2(Bu^t)]$ [a]	59.2

[a] Solution data for C_6D_6 solutions. [b] Solid-state spectrum. [c] DS = dehydroxylated silica.

Table II
Solution-Phase Catalytic Activity of $Cp'_2ThCH_3^+X^-$ Complexes[a]

reaction	$X^- = CH_3$	$^1/_2Fe(1,2\text{-}C_2B_9H_{11})_2^{2-}$	$B(C_6H_5)_4^-$	$B(C_6F_5)_4^-$
ethylene polymerization[b]	0	0	1.1×10^{-2}	36
1-hexene hydrogenation[c]	1.4×10^{-4}	0	1.1×10^{-3}	4.6

[a] As expressed in turnover frequencies (N_t, s^{-1}). Experimental procedures of ref 14. [b] $P_{ethylene}$ = 1.0 atm, T = 25 °C, solvent = toluene or benzene. [c] P_{H_2} = 1.0 atm, T = 25 °C, solvent = toluene or benzene.

this unusual surface phenomenology can be functionally modeled and elaborated upon in solution.

Model Cationic Organoactinide Chemistry in Solution

At the outset of this work (1984), little or no firm precedent existed for cationic species such as G in either conventional organoactinide or group 4 organometallic chemistry. Indeed, it was not clear whether such species could be prepared and, if so, whether they would exhibit the spectroscopic characteristics and extraordinary reactivity seen on the surfaces. Crucial design questions concern the selection of charge-compensating anion (X^- in M) and the preparative route. Regarding the former,

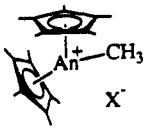

M

experience indicates that oxoanions (e.g., $CF_3SO_3^-$, ClO_4^-) with afford inert, covalent complexes[23] while conventional fluoro anions (e.g., BF_4^-, PF_6^-) will yield covalent complexes or undergo fluoride abstraction.[24] The ideal, minimally coordinating anion for a Cp'_2AnR^+ acid must have a sterically screening (to impede close cation–anion approach), charge-delocalized structure with nonpolar/noncoordinating peripheral substituents.[25] The preparative route must avoid coordinating

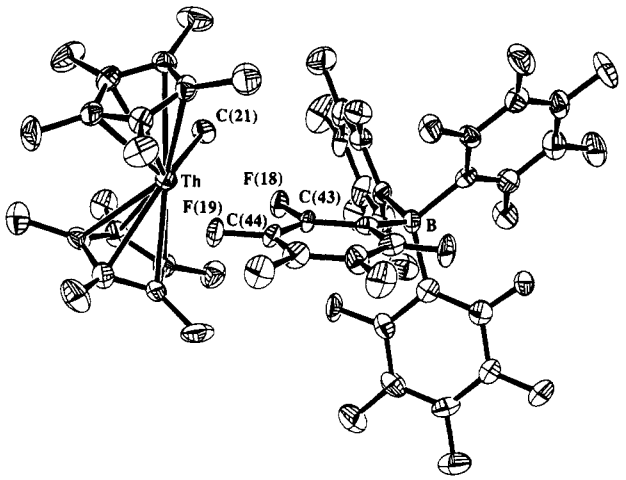

Figure 3. Molecular structure of $Cp'_2ThCH_3^+B(C_6F_5)_4^-$ (**1c**). Important bond distances (Å) and angles (deg) are as follows: Th–C(21) = 2.399 (8), Th–C_{ring} = 2.754 (3) (av), Th–F(18) = 2.757 (4), Th–F(19) = 2.675(5), C(43)–F(18) = 1.325 (6), C(44)–F(19) = 1.344 (7), and ring centroid–Th–ring centroid = 140.1 (3). Thermal ellipsoids are drawn at the 35% probability level (from ref 26a).

solvents and oxidizing agents.

We find that protonolytic reagents,[26] in the form of sterically encumbered ammonium salts, provide an efficacious route to $Cp'_2ThCH_3^+X^-$ complexes (eq 11).[27] Complexes **1b** and **1c** exhibit characteristic "cation-like"

$$Cp'_2Th(CH_3)_2 + R_3NH^+X^- \xrightarrow{\text{pentane}} \underset{\textbf{1a–c}}{Cp'_2ThCH_3^+X^-} + R_3N + CH_4 \quad (11)$$

R = *n*-butyl; **1a**, $X^- = {}^1/_2M(C_2B_9H_{11})_2^-$, M = Fe, Co; **1b**, $X^- = B(C_6H_5)_4^-$; **1c**, $X^- = B(C_6F_5)_4^-$

low-field Th–$^{13}CH_3$ signals (**1c** < **1b** < **1a**), which agree well with the surface spectroscopic data (Table I). However, **1a–c** differ enormously in solution reactivity for ethylene polymerization and 1-hexene hydrogenation (**1c** > **1b** ≫ **1a**; Table II), with *the reactivity of $Cp'_2ThCH_3^+B(C_6F_5)_4^-$ approaching the reactivity of the supported $Cp'_2Th(CH_3)_2$/DA catalyst.* The reasons for these marked reactivity differences appears to derive from the structural nature of the cation–anion interaction. The crystal structure of **1a** reveals close capping of dicarbollide faces by the $Cp'_2ThCH_3^+$ ions, with several close Th···H–B contacts.[28] Solid-state and low-temperature solution NMR data for **1b** suggest strong, coordinatively saturating π-arene complexation (e.g., N). In contrast, the crystal structure of **1c** (Figure

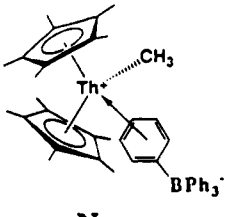

N

(22) (a) Bruno, J. W.; Marks, T. J.; Morss, L. R. *J. Am. Chem. Soc.* **1983**, *105*, 6824–6832. (b) Bruno, J. W.; Stecher, H. A.; Morss, L. R.; Sonnenberger, D. C.; Marks, T. J. *J. Am. Chem. Soc.* **1986**, *108*, 7275–7280.

(23) Toscano, P. J.; Marks, T. J. Unpublished observations.

(24) (a) Hitchock, P. B.; Lappert, M. F.; Taylor, R. G. *J. Chem. Soc., Chem. Commun.* **1984**, 1082–1084. (b) Honeychuck, R. V.; Hersh, W. H. *Inorg. Chem.* **1989**, *28*, 2869–2886 and references therein.

(25) For other approaches to weakly coordinating anions, see: (a) Moirot, M. D.; Anderson, O. P.; Strauss, S. H. *Inorg. Chem.* **1987**, *26*, 2216–2223 and referenes therein. (b) Liston, D. J.; Reed, C. A.; Eigenbrot, C. W.; Scheidt, W. R. *Inorg. Chem.* **1987**, *26*, 2739–2740 and references therein. (c) Beck, W.; Sünkel, K. *Chem. Rev.* **1988**, *88*, 1405–1421 and references therein. (d) Turner, H. W.; Hlatky, G. G. Eur. Pat. Appl. EP 211004, 1988.

(26) Lin, Z.; LeMarechal, J. F.; Sabat, M.; Marks, T. J. *J. Am. Chem. Soc.* **1987**, *109*, 4127–4129.

(27) (a) Yang, X.; Stern, C. L.; Marks, T. J. *Organometallics* **1991**, *10*, 840–842. (b) Yang, X.; Marks, T. J. Manuscript in preparation.

(28) Yang, X.; King, W. A.; Sabat, M.; Marks, T. J. Unpublished results.

3) consists of loosely associated "bent-sandwich" $Cp'_2ThCH_3^+$ cations and $B(C_6H_5)_4^-$ anions. Conspicuous in the former are the *short* Th–CH_3 and Th–C_{ring} distances. The shortest Th–F contacts (Th–F(18),F(19)) are significantly longer than the sums of relevant Th^{4+} and F^- ionic radii (~2.28 Å),[29] what has been assigned to a F→Yb dative bond[30] after correction for differences in Th^{4+}/Yb^{2+} ionic radii[30] (~2.29 Å), and a Th←O(THF) bond distance[26] after correction for differences in F/O covalent radii (~2.56 Å). The C-F(18),F(19) distances are unexceptional and the valence angles about the B atom essentially tetrahedral. In the solution ^{19}F NMR spectra, the C_6F_5 groups are in fast exchange down to −70 °C.

These results provide a compelling argument that G-type cation-like species are indeed formed on Lewis acidic surfaces by methide abstraction and that such species can exhibit high catalytic activity. Equally instructive is the finding that the reactivity of such cations exhibits a very large sensitivity to the nature of the charge-compensating anion, which is entirely consistent with the support-modulated adsorbate reactivity effects observed in the heterogeneous systems.

Group 4 Organometallic Surface Chemistry, Catalysis, and Spectroscopy

The foregoing discussion raises the question of whether such results are generalizable to the early transition metals, which form the basis for most current-generation olefin polymerization catalysts. Adsorption studies of $Cp_2Zr(CH_3)_2$, $Cp'_2Zr(CH_3)_2$, and $Cp'Zr(CH_3)_3$ have been carried out on alumina.[31] In general, evolved CH_4 yields on DA are comparable to those observed for $Cp'_2Th(CH_3)_2$/DA; however, CH_4 yields for adsorption on PDA are comparatively less. The explanation logically resides in the lower protonolytic reactivity and presumably lower polar character of Zr–alkyl bonds.[32]

In regard to heterogeneous catalysis, the order of activity for propylene hydrogenation and ethylene polymerization on DA again roughly parallels the coordinative unsaturation of the precatalyst:

$$Cp'Zr(CH_3)_3 > Cp_2Zr(CH_3)_2 > Cp'_2Zr(CH_3)_2$$

N_t for $Cp_2Zr(CH_3)_2$/DA-catalyzed propylene hydrogenation is ~30% of that for $Cp'_2Th(CH_3)_2$/DA. Poisoning experiments with CO indicate that ~4% of $Cp_2Zr(CH_3)_2$/DA and ~12% of $Cp'Zr(CH_3)_3$/DA surface sites are of catalytic significance. In marked contrast to the results for supported organoactinides, the above organozirconium complexes on *PDA* also exhibit significant activity for propylene hydrogenation: ca. 30% of that observed on DA. These results suggest strong parallels between the chemical properties of supported organo group 4 and organoactinide complexes, with a major divergence being the behavior on the partially hydroxylated support.

^{13}C CPMAS NMR studies[31] provide considerable insight into the above observations, while EPR measurements indicate reduction to Zr(III) to be insignificant. The NMR data show that the adsorption of $Cp_2Zr(^{13}CH_3)_2$ on DA proceeds analogously to that of $Cp'_2Th(^{13}CH_3)_2$ (eq 12). At the time of the first ex-

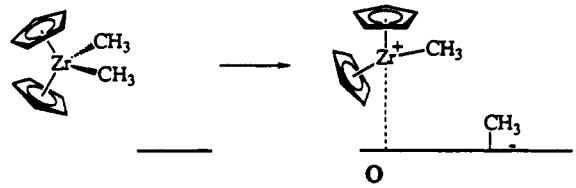

(12)

O

periment, the ^{13}C spectral parameters of O (both Zr–C_5H_5 and Zr–$^{13}CH_3$) were modeled reasonably well by those of known, *base-coordinated* cationic complexes of the type $Cp_2Zr(CH_3)L^+B(C_6H_5)_4^-$.[33] In agreement with the catalytic findings, the CPMAS spectra of $Cp_2Zr(^{13}CH_3)_2$/PDA show the presence of *both* μ-oxo species (e.g., P) and cations (O). Thus, zirconocene

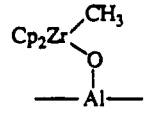

P

alkyl cations can also form on partially hydroxylated Lewis acidic surfaces, explaining the catalytic activities on such supports reported by other researchers,[3,4] and further strengthening the contention that Cp_2ZrR^+ adsorbate complexes are the catalytically active centers. Moreover, the observation of Lewis acid-promoted formation of cationic species accompanied by high activities for olefin hydrogenation and ethylene polymerization bears directly upon an important, unresolved issue in homogeneous Ziegler–Natta catalysis.

Model Cationic Organozirconium Chemistry in Solution

In addition to affording a better understanding of cationic adsorbate species (O), the synthesis of stable, base-free, highly electrophilic $Cp_2ZrR^+X^-$ complexes would offer models for several classes of important yet poorly understood, soluble olefin polymerization catalysts. Indirect evidence argues that catalysts prepared from metallocene dialkyls and large excesses of Lewis acid cocatalysts such as methylalumoxane ("$[Al(CH_3)O]_n$")[3,34] are in fact Cp_2ZrR^+ complexes.[35-41] If this is true, such chemistry would represent a direct parallel to the aforementioned organo group 4 surface chemistry.

Solution-phase models of eq 12 must conform to many of the guidelines set forth for $Cp'_2ThR^+X^-$ com-

(29) Shannon, R. D. *Acta Crystallogr., Sect. A* **1976**, *A32*, 751–767.
(30) Burns, C. J.; Anderson, R. A. *J. Chem. Soc., Chem. Commun.* **1989**, 136–137.
(31) (a) Dahmen, K. H.; Hedden, D.; Burwell, R. L., Jr.; Marks, T. J. *Langmuir* **1988**, *4*, 1212–1214. (b) Dahmen, K. H.; Burwell, R. L., Jr.; Marks, T. J. Manuscript in preparation.
(32) Schock, L. E.; Marks, T. J. *J. Am. Chem. Soc.* **1988**, *110*, 7701–7715 and references therein.
(33) Jordan, R. F.; Bagjur, C. S.; Willett, R.; Scott, B. *J. Am. Chem. Soc.* **1986**, *108*, 7410–7411.
(34) (a) Resconi, L.; Bossi, S.; Abis, L. *Macromolecules* **1990**, *23*, 4489–4491 and references therein. (b) Giannetti, E.; Nicoletti, G. M.; Mazzocchi, R. *J. Polym. Sci., Polymn. Chem. Ed.* **1985**, *23*, 2117–2133. (c) Kaminsky, W.; Lüker, H. *Makromol. Chem., Rapid Commun.* **1984**, *5*, 225–228 and references therein.
(35) Dyachkovskii, F. S.; Shilova, A. K.; Shilov, A. Y. *J. Polymn. Sci., Part C* **1967**, 2333–2339.
(36) Eisch, J. J.; Caldwell, C. J.; Werner, S.; Krüger, C. *Organometallics* **1991**, *10*, 3417–3419 and references therein.
(37) Jordan, R. F.; LaPointe, R. F.; Bradley, P. K.; Baenziger, N. *Organometallics* **1989**, *8*, 2892–2903 and references therein.
(38) Bochmann, M.; Jaggar, A. J.; Nicholls, J. C. *Angew. Chem., Int. Ed. Engl.* **1990**, *29*, 780–782 and references therein.
(39) Hlatky, G. G.; Turner, H. W.; Eckman, R. R. *J. Am. Chem. Soc.* **1989**, *111*, 2728–2729.
(40) Taube, R.; Krukowa, L. *J. Organomet. Chem.* **1988**, *347*, C9–C11.
(41) Gassman, P. G.; Callstrom, M. R. *J. Am. Chem. Soc.* **1987**, *109*, 7875–7876.

Table III
^{13}C NMR Data for Surface and Model Organozirconium Complexes

complex	δ Zr–$^{13}CH_3$ (ppm)
$Cp_2ZrCH_3^+CH_3B(C_6F_5)_3^-$ [a]	40.9
$Cp_2Zr(CH_3)_2$/MAO [b,c]	**41.3**
$Cp_2ZrCH_3(THF)^+B(C_6H_5)_4^-$ [a]	38.9
$Cp_2Zr(CH_3)_2$/DA [b]	**36.0**
$Cp_2Zr(CH_3)_2$ [a]	31.4
$Cp'_2ZrCH_3^+CH_3B(C_6F_5)_3^-$ [a]	50.4
$Cp'_2Zr(CH_3)_2$ [a]	36.2

[a] Solution spectrum in C_6D_6 solution. [b] Solid-state spectrum. [c] MAO = methylalumoxane.

plexes (vide supra). We sought a hydrocarbon-soluble, charge-delocalized organo Lewis acid devoid of nucleophilic/coordinating substituents. Using tris(pentafluorophenyl)borane, intermediate in Lewis acidity between BF_3 and BCl_3, the first stoichiometrically precise, isolable, crystallographically characterizable, highly active "cation-like" zirconocene polymerization catalysts were prepared (eq 13).[42] NMR spectroscopic

$$L_2Zr(CH_3)_2 + B(C_6F_5)_3 \xrightarrow{C_6H_6 \text{ or pentane}} L_2ZrCH_3^+CH_3B(C_6F_5)_3^- \quad (13)$$
2a–c

2a, L = η^5-C_5H_5; **2b**, L = η^5-1,2-$(CH_3)_2C_5H_3$; **2c**, L = η^5-$(CH_3)_5C_5$

properties of **2a** (δ Zr–C_5H_5 and δ Zr–CH_3) are remarkably similar to those of $Cp_2Zr(^{13}CH_3)_2$/DA as well as those of the zirconocene complex prepared in the reaction of $Cp_2Zr(CH_3)_2$ with methylalumoxane (Q, eq 14) (Table III).[43] Ethylene dosing studies of Q monitored by CPMAS NMR reveal insertion reactivity patterns similar to those found for $Cp'_2Th(^{13}CH_3)_2$/$MgCl_2$ (cf. Figure 2) except that ~100% of the zirconocene cation sites are reactive.[43]

$$Cp_2Zr(CH_3)_2 + \{Al(CH_3)O\}_n \rightleftarrows Cp_2ZrCH_3^+CH_3\{Al(CH_3)O\}_n^- \quad (14)$$
Q

The crystal structure of **2b** (Figure 4) consists of a "bent-sandwich" $[1,2\text{-}(CH_3)_2C_5H_3]_2ZrCH_3^+$ cation weakly coordinated to a $CH_3B(C_6F_5)_3^-$ anion via a nonlinear (161.8 (2)°), highly unsymmetrical Zr(μ-CH_3)B bridge. With the exception of a shortened Zr–C(15) bond, key aspects of the Zr coordination sphere are unexceptional. The Zr–CH_3(bridge) distance is elongated by ca. 0.3 Å, while the B–CH_3 distance is normal, and the valence angles about B deviate only slightly from tetrahedral. The C(34) hydrogen atoms are bent away from B and toward Zr, with the closest Zr···H contact (2.25 (3) Å) exceeding typical terminal and bridging Zr–H bond distances[44] as well as short Zr···H(C_{alkyl}) "agostic" distances.[45] It can also be seen that ion pair **2b** is dissymmetric (Figure 4), rendering the ring methyl groups (and ring 3,5 positions) magnetically nonequivalent (diastereotopic). Dynamic

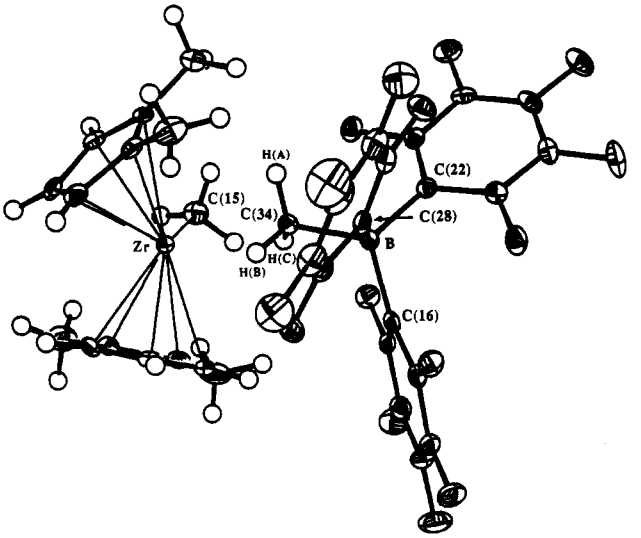

Figure 4. Molecular structure of $[1,2\text{-}(CH_3)_2C_5H_3]_2ZrCH_3^+$-$CH_3B(C_6F_5)_3^-$ (**2b**). Important bond distances (Å) and angles (deg) are as follows: Zr–C(15) = 2.252 (4), Zr–C(34) = 2.549 (3), B–C(34) = 1.663 (5), Zr–H(34A) = 2.71 (3), Zr–H(34B) = 2.25 (3), Zr–H(34C) = 2.30 (3), Zr–C_{ring} = 2.500 (1) (av), ∠C(15)–Zr–C(34) = 92.0 (1), ∠C(16)–B–C(34) = 108.7 (3), ∠C(22)–B–C(34) = 112.7 (2), ∠C(28)–B–C(34) = 102.8 (3), ∠C(16)–B–C(22) = 106.5 (3), ∠C(16)–B–C(28) = 114.3 (3), ∠C(22)–B–C(28) = 112.0 (3). Thermal ellipsoids are drawn at the 35% probability level (from ref 41a).

NMR spectroscopy can be employed to probe B–CH_3 bond lability and the tightness of the ion pairing in **2b**, since symmetrizing processes which are fast on the NMR time scale can be readily detected. We find that reorganization of the ion pair structures occurs slightly more rapidly (~5×) than transposition of the triarylborane coordination. The barriers to both processes are appreciable ($\Delta G^{\ddagger} \approx 19$ kcal/mol).

Complexes **2a–c** are active catalysts for homogeneous olefin polymerization. Ethylene polymerization proceeds at 25 °C, 1 atm of pressure, with N_t(**2a**) ≈ 45 s^{-1} (~4.5 × 10^6 g of polyethylene (mol of Zr)$^{-1}$ h^{-1} atm^{-1}), comparable in activity to typical zirconocene/alumoxane catalysts.[34] With propylene at 25 °C, **2a** yields atactic polypropylene with $N_t(1) \approx 4.2$ s^{-1} ($\bar{M}_w$ = 15600; $\bar{M}_n$ = 3000). NMR experiments in which a toluene-d_8 solution of **2a** is exposed to 5 equiv of propylene at −25 °C indicate that >70% of **2a** undergoes olefin insertion under these conditions, arguing that the observed activity is not due to a minor component.

Concluding Remarks

This research has shown that strong parallels can be drawn between the surface organometallic chemistry and catalytic properties of adsorbed actinide/group 4 hydrocarbyls and certain classes of solution-phase molecules. CPMAS NMR spectroscopy shows that alkyl anion abstraction constitutes a major adsorptive pathway on dehydroxylated Lewis acidic supports. The resulting cation-like species are highly active heterogeneous catalysts for olefin hydrogenation and ethylene polymerization. The catalytic behavior is a strong function of the nature of the charge-compensating support material and likely the local surface topology. On hydroxylated supports, μ-oxo adsorbate species are formed which are catalytically inactive. Using solution-phase protonolytic or organo Lewis acid abstractive approaches, it is possible to synthesize crystallographically characterizable, cation-like spectroscopic, struc-

(42) (a) Yang, X.; Stern, C. L.; Marks, T. J. *J. Am. Chem. Soc.* **1990**, *113*, 3623–3625. (b) Yang, X.; Cohen, J. W.; Marks, T. J. Unpublished results.
(43) Sishta, C.; Hathorn, R. M.; Marks, T. J. *J. Am. Chem. Soc.*, in press.
(44) Jones, S. B.; Petersen, J. L. *Inorg. Chem.* **1981**, *20*, 2889–2894.
(45) Jordan, R. F.; Bradley, P. K.; Baenziger, N. C.; La Pointe, R. E. *J. Am. Chem. Soc.* **1990**, *112*, 1289–1291.

tural, and functional models for the aforementioned adsorbate species. The reactivity of these ion pairs is strongly dependent upon the coordinative properties of the charge-compensating anion, in agreement with the support sensitivities seen in the heterogeneous systems. The most loosely connected ion pairs are extremely reactive, with catalytic activities approaching those of the supported catalysts. Moreover, the soluble group 4 complexes can serve as stoichiometrically precise models for several important classes of alumoxane-based olefin polymerization catalysts. These results show that exciting opportunities exist where heterogeneous catalysis can teach us new things about homogeneous catalysis and vice versa. The challenge lies in building bridges between the two areas using the appropriate physicochemical techniques and synthetic strategies.

This research would not have been possible without the generous support of the U.S. Department of Energy under Grant DE-FG02-86ER13511. I am truly fortunate to have enjoyed the collaboration of a group of enthusiastic and talented colleagues. Their names can be found in the references.

Molecular Quantum Beats. High-Resolution Spectroscopy in the Time Domain

HERBERT BITTO and J. ROBERT HUBER*

Physikalisch-Chemisches Institut der Universität Zürich, Winterthurerstrasse 190, CH-8057 Zürich, Switzerland

Received April 15, 1991 (Revised Manuscript Received November 4, 1991)

Chemistry is the world of molecules, and within this world the chemical reaction is one of the most important parts, if not the most important. How molecules decay and how they react with other molecules on a microscopic basis is of most interest to the chemist.[1] The understanding of chemical reactions requires, however, a very detailed knowledge of the molecular electronic structure, for even its smallest features can have a decisive influence on the dynamics of such complex systems as molecules. The exploration of the atomic and molecular electronic structure has benefited greatly from high-resolution spectroscopy, which has progressed considerably since the advent of the laser by taking advantage of the unique laser properties such as monochromaticity, high intensity, and extremely short pulses. The rapid development of the laser has produced state-of-the-art systems whose characteristics are close to the limits imposed by physical laws. With respect to the frequency domain, continuous-wave lasers nowadays feature bandwidths well below 1 kHz whereas, with respect to the time domain, pulses as short as 6 fs have been successfully generated. So it seems that narrow-band laser radiation should allow spectroscopists to resolve spectra of molecules in the gas phase to nearly any desired extent while the extremely short pulses may be used to reveal the dynamics of atomic motion in a molecule. This remarkable radiation of "purest color" is available, and even this is tunable. However, it is not the light source that limits the resolution but the simple fact that the motion of the freely moving gas molecules causes line broadening in the spectra due to the Doppler effect.

Several spectroscopic methods have been developed to overcome Doppler broadening, for example, nonlinear techniques such as saturation spectroscopy, polarization spectroscopy, or two-photon spectroscopy with counterpropagating laser beams, as well as simple reduction of the molecules' velocity spread in molecular beams. Another method, conceptually very fundamental and experimentally relatively inexpensive, is based on the quantum beat phenomenon. Quantum beats appear as oscillations superimposed on the time-resolved fluorescence after a laser pulse has excited within its energy uncertainty two or more states in an atom or molecule. The frequencies of the quantum beats are just the energy differences between the "coherently" excited states.

This effect, lying at the heart of quantum mechanics, was introduced to atomic spectroscopy by Alexandrov and by Dodd and co-workers in 1964, but only with the introduction of the pulsed laser have quantum beats become interesting for a spectroscopic application.[2] It is the aim of this Account to give a short and simple description of just this phenomenon and to show how it is utilized as a high-resolution, molecular spectroscopic technique in the time domain, going far beyond rotational resolution.[3-5] The power and versatility of quantum beat spectroscopy will then be demonstrated

Herbert Bitto was born in Hakducica, Yugoslavia, on June 13, 1954 and received his Pd.D. from the University of Zürich (1984). He spent two years as a NATO postdoctoral fellow at the University of California, Berkeley. Since 1986 he has been Research Associate at the University of Zürich and head of the computer-assisted experimentation facility of the Institute of Physical Chemistry. His interests in research as well as in music include everything that has "rhythm and beat".

J. Robert Huber was born in Zürich, Switzerland, on October 29, 1934 and received his Ph.D. (1966) from the Swiss Federal Institute of Technology (ETH) in Zürich. He was a postdoctoral fellow with the US Army Pioneering Research Labs in Natick, MA, and then joined the faculty at Northeastern University in Boston. In 1973 he became Professor of Chemistry at the University of Konstanz, Germany, and in 1979 assumed his current position as chaired Professor of Physical Chemistry at the University of Zürich. His research centers on molecular dynamics, laser spectroscopy, and photochemistry.

(1) Levine, R. D.; Bernstein, R. B. *Molecular Reaction Dynamics and Chemical Reactivity*; Oxford University Press: Oxford, 1987. Dixon, R. N. *Acc. Chem. Res.* **1991**, *24*, 16.
(2) Haroche, S. In *High-Resolution Laser Spectroscopy*; Shimoda, K., Ed.; Springer-Verlag: Berlin, 1976.
(3) Chaiken, J.; Benson, T.; Gurnick, M.; McDonald, J. D. *Chem. Phys. Lett.* **1979**, *61*, 195. Chaiken, J.; Gurnick, M.; McDonald, J. D. *J. Chem. Phys.* **1981**, *74*, 106.
(4) Bitto, H.; Huber, J. R. *Opt. Commun.* **1990**, *80*, 184.
(5) Hack, E.; Huber, J. R. *Int. Rev. Phys. Chem.* **1991**, *10*, 287.

0001-4842/92/0125-0065$03.00/0